

A Max-Sum algorithm for training discrete neural networks

Carlo Baldassi

*DISAT, Politecnico di Torino, Corso Duca Degli Abruzzi 24, 10129 Torino and
Human Genetics Foundation, Via Nizza 52, 10124 Torino*

Alfredo Braunstein

*DISAT, Politecnico di Torino, Corso Duca Degli Abruzzi 24, 10129 Torino
Human Genetics Foundation, Via Nizza 52, 10124 Torino and
Collegio Carlo Alberto, Via Real Collegio 1, Moncalieri*

We present an efficient learning algorithm for the problem of training neural networks with discrete synapses, a well-known hard (NP-complete) discrete optimization problem. The algorithm is a variant of the so-called Max-Sum (MS) algorithm. In particular, we show how, for bounded integer weights with q distinct states and independent concave *a priori* distribution (e.g. l_1 regularization), the algorithm's time complexity can be made to scale as $O(N \log N)$ per node update, thus putting it on par with alternative schemes, such as Belief Propagation (BP), without resorting to approximations. Two special cases are of particular interest: binary synapses $W \in \{-1, 1\}$ and ternary synapses $W \in \{-1, 0, 1\}$ with l_0 regularization. The algorithm we present performs as well as BP on binary perceptron learning problems, and may be better suited to address the problem on fully-connected two-layer networks, since inherent symmetries in two layer networks are naturally broken using the MS approach.

CONTENTS

I. Introduction		2
II. The network model		5
III. The Max-Sum algorithm		7
A. Max Convolution		9
B. The binary case		13
IV. Numerical results		16
V. Conclusions		18
Acknowledgments		20
Appendix		20
Details of the computation of the cavity fields.		20
References		23

I. INTRODUCTION

The problem of training an artificial, feed-forward neural network in a supervised way is a well-known optimization problem, with many applications in machine learning, inference etc. In general terms, the problem consists in obtaining an assignment of “synaptic weights” (i.e. the parameters of the model) such that the device realizes a transfer function which achieves the smallest possible error rate when tested on a given dataset of input-output examples. Time is usually assumed to be discretized. In a single-layer network, the transfer function is typically some non-linear function (e.g. a sigmoid or a step function) of the scalar product between a vector of inputs and the vector of synaptic weights. In multi-layer networks, many single-layer units operate in parallel on the same inputs, and their outputs provide the input to

other similar (with a varying degree of similarity) units, until the last layer is reached.

The most popular and successful approaches to these kind of optimization problems are typically variants of the gradient descent algorithm, and in particular the back-propagation algorithm [1]. On single-layer networks with simple non-linearities in their output functions these algorithms can even be shown to achieve optimal results in linear time [2]; on multi-layer networks these algorithms suffer from the usual drawbacks of gradient descent (mostly the presence of local minima, and slow convergence under some circumstances).

On the other hand, gradient descent can only be applied to continuous problems. If the synaptic weights are restricted to take only discrete values, the abovementioned family of methods can not be applied; in fact, it is known that even the simplest version of the problem (classification using a single-layer network) becomes computationally hard (NP-complete) in the worst-case scenario [3, 4]. However, some theoretical properties of the networks, such as the storage capacity (i.e. the amount of information which can be effectively stored in the device by setting the synaptic weights), are only slightly worse in the case of discrete synapses, and other properties (e.g. robustness to noise and simplicity) would make them an attractive model for practical applications. Indeed, some experimental results [5–7], as well as arguments from theoretical studies and computer simulations [8–11], suggest that long term information storage may be achieved by using discrete — rather than continuous — synaptic states in biological neural networks.

Therefore, the study of neural network models with discrete weights is interesting both as a hard combinatorial optimization problem and for its potential applications, in practical implementations as well as for modeling biological networks. On the theoretical side, some light has been shedded upon the origin of the computational hardness in these kind of problems by the study of the space of the solutions by means of methods derived from Statistical Physics approaches [12, 13]: in brief, most solutions are isolated, i.e. far from each other, and the energy landscape is riddled with local minima which tend to trap purely local search methods, which thus show very poor performance. On the application side, a family of heuristic algorithms, derived from the cavity method, have been devised, which exhibit very good performance on random instances, both in terms of solution time and in terms of scaling with the

size of the problem.

In particular, it was first shown in [14] that a version of the Belief Propagation (BP) algorithm [15] with the addition of a reinforcement term was able to efficiently solve the problem of correctly classifying αN random input-output associations using a single-layer network, or a tree-like two-layer network, with N synapses, up to a value of α close to the theoretical upper bound. For the single-layer case, the theoretical bound for binary synapses is $\alpha_c \simeq 0.83$ [12], while the algorithmic bound as estimated from extensive simulations up to $N = 10^6$ is $\alpha_{BP} \simeq 0.74$. Two more algorithms, obtained as crudely simplified versions of the reinforced BP, were later shown [16, 17] to be able to achieve very similar performances, despite being simpler and working in an on-line fashion. The time complexity of all these algorithms was measured to be of order $N\sqrt{\log N}$ per pattern; the BP algorithm in particular achieves this performance thanks to a Gaussian approximation which is valid at large N .

When considering multi-layer networks, the original BP approach of [14] can only effectively deal with tree-like network structures; fully-connected structures (such as those commonly used in machine learning tasks) can not be addressed (at least not straightforwardly) with this approach, due to strong correlations arising from a permutation symmetry which emerges in the second layer.

In this paper, we present a new algorithm for addressing the problem of supervised training of network with binary synapses. The algorithm is a variant of the so-called Max-Sum algorithm (MS) [15] with an additional reinforcement term (analogous to the reinforcement term used in [14]). The MS algorithm is a particular zero-temperature limit of the BP algorithm; but it should be noted that this limit can be taken in different ways. In particular, the BP approach in [14] was applied directly at zero temperature as patterns had to be learned with no errors. In the MS approach we present here, in addition to hard constraints imposing that no errors are made on the training set, we add external fields with a temperature that goes to zero in a second step. Random small external fields also break the permutation symmetry for multi-layer networks.

In the MS approach, the Gaussian approximation which is used in the BP approach can not be used, and a full convolution needs to be computed instead: this in principle would add a factor of N^2 to the time complexity, but, as we shall show, the exploitation of the convexity properties of the problem allows

to simplify this computation, reducing the additional factor to just $\log N$.

This reinforced MS algorithm has very similar performance to the reinforced BP algorithm on single layer networks in terms of storage capacity and of time required to perform each node update; however, the number of updates required to reach a solution scales polynomially with N , thus degrading the overall scaling. On fully-connected multi-layer networks, the MS algorithm performs noticeably better than BP.

The rest of the paper is organized as follows: in Section II we present the network model and the mathematical problem of learning. In Section III we present the MS approach for discrete weights. We show how the inherent equations can be solved efficiently thanks to properties of the convolution of concave piecewise-linear functions, and describe in complete detail the implementation for binary weights. Finally, in Section IV we show simulation results for the single and two-layer case.

II. THE NETWORK MODEL

We consider networks composed of one or more elementary “building blocks” (units), each one having a number of discrete weights and a binary transfer function, which classify binary input vectors. Units can be arranged as a composed function (in which the output from some units is considered as the input of others) in various ways (also called architectures) that is able to produce a classification output from each input vector.

We denote the input vectors as $\xi^\mu = \{\xi_i^\mu\}_{i=1,\dots,N} \in \{-1, +1\}^N$ (where μ is a pattern index) and the weights as $W^k = \{W_i^k\}_{i=1,\dots,N}$ (where k is a unit index). In the following, the W_i^k are assumed to take q evenly spaced values; we will then explicitly consider the cases $q = 2$ with $W_i^k \in \{-1, 1\}$ and $q = 3$ with $W_i^k \in \{-1, 0, 1\}$. The output of the unit is given by:

$$\sigma^{k\mu} = \text{sign} \left(\sum_{i=1}^N W_i^k \xi_i^\mu \right) \quad (1)$$

with the convention that $\text{sign}(0) = 1$.

We will consider two cases: a single layer network and two-layer comitee machine. In single-layer networks, also called perceptrons [18], there is a single unit, and therefore we will omit the index k . Fully

connected two-layer networks consist of K units in the second layer, each of which receives the same input vector ξ^μ , and the output function of the device is

$$\sigma^\mu = \text{sign} \left(\sum_{k=1}^K \sigma^{k\mu} \right)$$

This kind of architecture is also called a committee or consensus machine [19]. When $K = 1$, this reduces to the perceptron case. In a tree-like committee machine the input vectors would not be shared among the units; rather, each unit would only have access to a subset of the input vectors, without overlap between the units. For a given N , the tree-like architectures are generally less powerful (in terms of computational capabilities or storage capacity) than the fully-connected ones, but are easier to train [20]. Intermediate situations between these two extremes are also possible. In fully-connected committee machines there is a permutation symmetry in the indices k , since any two machines which only differ by a permutation of the second layer's indices will produce the same output.

Throughout this paper we will consider supervised contexts, in which each pattern μ has an associated desired output σ_D^μ .

In *classification* (or *storage*) problems, $M = \alpha NK$ association pairs of input vectors ξ^μ and corresponding desired outputs σ_D^μ are extracted from some probability distribution, and the goal is to find a set of weights $\{W^k\}_k$ such that $\forall \mu \in \{1, \dots, \alpha NK\} : \sigma^\mu = \sigma_D^\mu$.

In random *generalization* problems, the input patterns ξ^μ are still extracted from some probability distribution, but the desired outputs σ_D^μ are computed from some rule, usually from a teacher device (*teacher-student* problem). The goal then is to learn the rule itself, i.e. to achieve the lowest possible error rate when presented with a pattern which was never seen during the training phase. If the teacher's architecture is identical to that of the student device, this can be achieved when the student's weights match those of the teacher (up to a permutation of the units' indices in the fully-connected case).

In the following, we will always address the problem of minimizing the error function on the training

patterns:

$$\begin{aligned}
E\left(\left\{W^k\right\}_k\right) &= \sum_{\mu=1}^{\alpha N} E_{\mu}\left(\left\{W^k\right\}_k\right) - \sum_i \Gamma_i^k\left(W_i^k\right) \\
&= \sum_{\mu=1}^{\alpha N} \Theta\left(-\sigma_D^{\mu} \operatorname{sign}\left(\sum_{k=1}^K \operatorname{sign}\left(\sum_{i=1}^N W_i^k \xi_i^{\mu}\right)\right)\right) - \sum_i \Gamma_i^k\left(W_i^k\right)
\end{aligned} \tag{2}$$

where $\Theta(x)$ is the Heaviside step function $\Theta(x) = 1$ if $x > 0$ and 0 otherwise. The term $\Gamma_i^k(W_i^k)$ has the role of an external field, and can be used e.g. to implement a regularization scheme; in the following, we will always assume it to be concave. For example we can implement l_1 regularization by setting $\Gamma_i^k(W_i^k) = -\lambda|W_i^k|$ where $\lambda > 0$ is a parameter. The first term of expression (2) therefore counts the number of misclassified patterns and the second one favours sparser solutions.

Throughout the paper, all random binary variables are assumed to be extracted from an unbiased i.i.d. distribution.

Under these conditions, it is known that in the limit of $N \gg 1$ there are phase transitions at particular values of α . For single units (perceptrons) with binary ± 1 synapses, for the classification problem, the minimum number of errors is typically 0 up to $\alpha_c \simeq 0.83$. For the generalization problem, the number of devices which are compatible with the training set is larger than 1 up to $\alpha_{TS} \simeq 1.245$, after which the teacher perceptron becomes the only solution to the problem.

III. THE MAX-SUM ALGORITHM

Following [14], we can represent the optimization problem of finding the zeros of the first term of eq. (2) on a complete bipartite factor graph. Starting from the single-layer case, the graph has N vertices (variable nodes) representing the W_i values and αN factor nodes representing the error terms $E_{\mu}(\mathbf{W})$.

The standard MS equations for this graph involve two kind of messages associated with each edge of the graph; we indicate with $\Phi_{\mu \rightarrow i}^t(W_i)$ the message directed from node μ to variable i at time step t , and with $\Psi_{i \rightarrow \mu}^t(W_i)$ the message directed in the opposite direction.

These messages represent a certain zero-temperature limit of BP messages, but have also a direct interpretation in terms of energy shifts of modified systems. Disregarding an insubstantial additive constant,

message $\Phi_{\mu \rightarrow i}(W_i)$ represents the negated energy (2) restricted to solutions taking a specific value W_i for variable i , on a modified system in which the energy depends on W_i only through the factor node μ , i.e. in which all terms $W_i \xi_i^\nu$ for all $\nu \neq \mu$ are removed from the energy expression (2). Similarly, message $\Psi_{i \rightarrow \mu}^t(W_i)$ represents an analogous negated energy on a modified system in which the term E_μ is removed. For factor graphs that are acyclic, the MS equations can be thought of as the dynamic programming exact solution. In our case, the factor graph, being complete bipartite, is far from being acyclic and the equations are only approximate. For BP, the approximation is equivalent to the one of the Thouless-Anderson-Palmer's equations [21] and is expected to be exact in the single-layer case below the critical capacity [12]. For a complete description of the MS equations and algorithm, see [15].

The MS equations [15] for energy (2) are:

$$\Phi_{\mu \rightarrow i}^{t+1}(W_i) = \max_{\{W_j\}_{j \neq i}: E_\mu(\mathbf{W})=0} \left(\sum_{j \neq i} \Psi_{j \rightarrow \mu}^t(W_j) \right) - Z_{\mu \rightarrow i}^{t+1} \quad (3)$$

$$\Psi_{i \rightarrow \mu}^t(W_i) = \Gamma_i(W_i) + \sum_{\mu' \neq \mu} \Phi_{\mu' \rightarrow i}^t(W_i) - Z_{i \rightarrow \mu}^t \quad (4)$$

where $Z_{\mu \rightarrow i}^t$ and $Z_{i \rightarrow \mu}^t$ are normalization scalars that ensure $\sum_{W_i} \Psi_{i \rightarrow \mu}^t(W_i) = \sum_{W_i} \Phi_{\mu \rightarrow i}^t(W_i) = 0$ and can be computed after the rest of the RHS. At any given time t , we can compute the single-site quantities

$$\Psi_i^t(W_i) = \Gamma_i(W_i) + \sum_{\mu} \Phi_{\mu \rightarrow i}^t(W_i) - Z_i^t \quad (5)$$

and use them to produce an assignment of the \mathbf{W} 's:

$$W_i^t = \operatorname{argmax}_{W_i} \Psi_i^t(W_i) \quad (6)$$

The standard MS procedure thus consists in initializing the messages $\Psi_{i \rightarrow \mu}^0(W_i)$, iterating eqs. (3) and (4) and, at each time step t , computing a vector W^t according to eqs. (5) and (6) until either $E(W^t) = 0$ (in the absence of prior terms, i.e. when $\lambda = 0$), or the messages converge to a fixed point, or some maximum iteration limit is reached.

Strictly speaking, standard MS is only guaranteed to reach a fixed point if the factor graph is acyclic, which is clearly not the case here. Furthermore, if the problem has more than one solution (ground state),

the assignment in eq. (6) would not yield a solution even in the acyclic case. In order to (heuristically) overcome these problems, we add a time-dependent reinforcement term to eqs. (4) and (5), analogously to what is done for BP [14]:

$$\Psi_{i \rightarrow \mu}^t(W_i) = r t \Psi_i^{t-1}(W_i) + \Gamma_i(W_i) + \sum_{\mu' \neq \mu} \Phi_{\mu' \rightarrow i}^t(W_i) - Z_{i \rightarrow \mu}^t \quad (7)$$

$$\Psi_i^t(W_i) = r t \Psi_i^{t-1}(W_i) + \Gamma_i(W_i) + \sum_{\mu'} \Phi_{\mu' \rightarrow i}^t(W_i) - Z_i^t \quad (8)$$

where $r > 0$ controls the reinforcement speed. This reinforcement term in the case of standard BP implements a sort of “soft decimation” process, in which single variable marginals are iteratively pushed to concentrate on a single value. For the case of MS, this process is useful to aid convergence: on a system in which the MS equations do not converge, the computed MS local fields still give some information about the ground states and can be used to iteratively “bootstrap” the system into one with very large external fields, i.e. fully polarized on a single configuration [22]. The addition of this term introduces a dependence on the initial condition. Experimentally, by reducing r this dependence can be made arbitrarily small, leading to more accurate results (see Sec. IV), at the cost of increasing the number of steps required for convergence; our tests show that the convergence time scales as r^{-1} .

Furthermore, in order to break symmetries between competing configurations, we add a small symmetry-breaking concave noise $\Gamma'_i(W_i) \ll 1$ to the external fields $\Gamma_i(W_i)$; this, together with the addition of the reinforcement term, is sufficient to ensure — for all practical purposes — that the argmax in (6) is unique at every step of the iteration.

A. Max Convolution

While Eq. (7) can be efficiently computed in a straightforward way, the first term of Eq. (3) involves a maximum over an exponentially large set. The computation of Eq. (3) can be rendered tractable by adding $0 = \max_{\Delta} L\left(\Delta, \sum_{j \neq i} \xi_j^{\mu} W_j\right)$ where $L(x, y)$ is equal to 0 if $x = y$ and $-\infty$ otherwise, which leads to the following transformations:

$$\begin{aligned}
\Phi_{\mu \rightarrow i}^{t+1}(W_i) + Z_{\mu \rightarrow i}^{t+1} &= \max_{\{W_j\}_{j \neq i}: E_\mu(\mathbf{W})=0} \left(\sum_{j \neq i} \Psi_{j \rightarrow \mu}^t(W_j) \right) \\
&= \max_{\{W_j\}_{j \neq i}: E_\mu(\mathbf{W})=0} \left\{ \max_{\Delta} L \left(\Delta, \sum_{j \neq i} \xi_j^\mu W_j \right) + \sum_{j \neq i} \Psi_{j \rightarrow \mu}^t(W_j) \right\} \\
&= \max_{\Delta: \sigma_D^\mu(\Delta + \xi_i^\mu W_i) \geq 0} \left\{ \max_{\{W_j\}_{j \neq i}: \sum_{j \neq i} \xi_j^\mu W_j = \Delta} \sum_{j \neq i} \Psi_{j \rightarrow \mu}^t(W_j) \right\} \\
&= \max_{\Delta: \sigma_D^\mu(\Delta + \xi_i^\mu W_i) \geq 0} \mathcal{F}_{\mu \rightarrow i}^t(\Delta), \tag{9}
\end{aligned}$$

where in the last step above $\mathcal{F}_{\mu \rightarrow i}^t(\Delta)$ is defined as:

$$\mathcal{F}_{\mu \rightarrow i}^t(\Delta) = \max_{\{S_j\}_{j \neq i}: \sum_{j \neq i} S_j = \Delta} \left(\sum_{j \neq i} \Psi_{j \rightarrow \mu}^t(S_j \xi_j^\mu) \right). \tag{10}$$

The right-hand side of (10) is usually called a ‘‘Max-Convolution’’ of the functions $f_j(S_j) = \Psi_{j \rightarrow \mu}(S_j \xi_j^\mu)$ for $j \neq i$, and is analogous to the standard convolution but with operations $(\max, +)$ substituting the usual $(+, \times)$. As standard convolution, the operation is associative, which allows to compute the convolution of the $N - 1$ functions in a recursive way. As the convolution of two functions with discrete domains $\{0, \dots, q_1\}$ and $\{0, \dots, q_2\}$ respectively can be computed in $q_1 q_2$ operations and has domain in $\{0, \dots, q_1 + q_2\}$, it follows that (10) can be computed in $O(N^2)$ operations. In principle, this computation must be performed N times for each pattern μ to compute all $\Phi_{\mu \rightarrow i}$ messages, in a total of time $O(N^3)$.

A technique like the one described in [23–25] can be employed to reduce this by a factor N , coming back again to $O(N^2)$ operations per pattern update, as follows. Precomputing the partial convolutions L_n and R_n of f_1, \dots, f_n and f_n, \dots, f_N (respectively) for every n in $1, \dots, N$ can be done using N^2 operations in total; then the convolution of $\{f_j\}_{j \neq i}$ can be computed as the convolution of L_{i-1} and R_{i+1} . Computing this convolution would require $O(N^2)$ operations but fortunately this will not be needed; the

computation of (9) can proceed as:

$$\begin{aligned}
\Phi_{\mu \rightarrow i}^{t+1}(W_i) + Z_{\mu \rightarrow i}^{t+1} &= \max_{\Delta: \sigma_D^\mu(\Delta + \xi_i^\mu W_i) \geq 0} \left\{ \max_z L_{i-1}(z) + R_{i+1}(\Delta - z) \right\} \\
&= \max_z \left\{ L_{i-1}(z) + \max_{\Delta: \sigma_D^\mu(\Delta + \xi_i^\mu W_i) \geq 0} R_{i+1}(\Delta - z) \right\} \\
&= \max_z \left\{ L_{i-1}(z) + R_{i+1}^{\sigma_D^\mu}(z + \xi_i^\mu W_i) \right\} \tag{11}
\end{aligned}$$

where we defined $R_i^\sigma(x) = \max_{\Delta: \sigma(\Delta+x) \geq 0} R_i(\Delta)$. As the vectors R_i^σ can be pre-computed recursively in a total time of $\mathcal{O}(N^2)$ and (11) requires time $\mathcal{O}(N)$, we obtain a grand total $\mathcal{O}(N^2)$ operations per pattern update, or $\mathcal{O}(MN^2)$ per iteration. Unfortunately, this scaling is normally still too slow to be of practical use for moderately large values of N and we will thus proceed differently by exploiting convexity properties. However, note that the above scaling is still the best we can achieve for the general case in which regularization terms are not concave.

At variance with standard discrete convolution, in general Max-Convolution does not have an analogous to the Fast Fourier Transform, that would allow a reduction of the computation time of a convolution of functions with $\mathcal{O}(N)$ values from N^2 to $N \log N$. Nevertheless, for concave functions the convolution can be computed efficiently, as we will show below. Note that for this class of functions, an operation that is analogous to the Fast Fourier Transform is the Legendre-Fenchel transform [26], though it will be simpler to work with the convolution directly in the original function space.

First, let us recall well-known results about max-convolution of concave piecewise-linear functions in the family $\mathcal{C} = \{f: \mathbb{R}_{\geq 0} \rightarrow \mathbb{R} \cup \{-\infty\}\}$ [26]. First, the max-convolution $f_{12} \stackrel{\text{def}}{=} f_1 \otimes f_2$ of $f_1, f_2 \in \mathcal{C}$ belongs to \mathcal{C} . Moreover, $f_1 \otimes f_2$ can be built in an efficient way from f_1 and f_2 . Start with $x_1^{12} \stackrel{\text{def}}{=} \inf \{x: (f_1 \otimes f_2)(x) > -\infty\}$, which is easily computed as $x_1^{12} = x_1^1 + x_1^2$ with $x_1^i = \inf \{x: f_i(x) > -\infty\}$. Moreover, $(f_1 \otimes f_2)(x_1^{12}) = f_1(x_1^1) + f_2(x_1^2)$. Then, order the set of linear pieces from f_1 and f_2 in decreasing order of slope and place them in order, starting from $(x_1^{12}, f(x_1^{12}))$ to form a piecewise-linear continuous function. The method is sketched in Fig. 1. In symbols, let us write each concave piecewise-linear function $f_i(x)$ when $x \geq x_1^i$ as:

$$f_i(x) = \sum_{j=1}^{k_i} (x - x_j^i)_+ a_j^i + f_i(x_1^i) \quad i = 1, 2$$

with $a_j^i \in [0, \infty]$ for $j = 2, \dots, k_i$ and $x_1^i < x_2^i < \dots < x_{k_i}^i$. Here we used the notation [27] $y_+ = \frac{1}{2}(|y| + y)$. This function is concave, as for $x \in [x_j^i, x_{j+1}^i]$ the slope is $b_j^i = \sum_{k=1}^j a_k^i$ that is clearly decreasing with j . To compute the convolution of f_1 and f_2 , just order the slopes b_j^i ; i.e. compute a one to one map $\pi : (i, j) \mapsto c$ from couples $i \in \{1, 2\}, 1 \leq j \leq k_i$ to integers $1 \leq c \leq k_1 + k_2$ such that $\pi(i, j) < \pi(i', j')$ implies $b_j^i > b_{j'}^{i'}$. The max convolution for $x \geq x_1^{12}$ is still concave and piecewise-linear, and thus it can be written as:

$$(f_1 \otimes f_2)(x) = \sum_{c=1}^{k_{12}} (x - x_c^{12})_+ a_c^{12} + (f_1 \otimes f_2)(x_1^{12})$$

where $k_{12} = k_1 + k_2 - 1$. For each c we can retrieve $(i(c), j(c)) = \pi^{-1}(c)$; with this, the parameters of the convolution are $a_1^{12} = b_{j(1)}^{i(1)}$, $a_{c+1}^{12} = b_{j(c+1)}^{i(c+1)} - b_{j(c)}^{i(c)}$ and $x_{c+1}^{12} = x_1^{12} + x_{j(c)+1}^{i(c)} - x_{j(c)}^{i(c)}$.

For more details about the max-convolution of piecewise-linear concave functions, see e.g. [26, Part II].

We now consider the case of functions defined on a discrete domain. Let f, g be concave discrete functions in

$$\mathcal{D} = \{f : \{0, \dots, q-1\} \rightarrow \mathbb{R} \cup \{-\infty\}\}$$

We will define the continuous extension $\hat{f} \in \mathcal{C}$ as the piecewise-linear interpolation of f , with value $-\infty$ for arguments in $(-\infty, 0) \cup (q-1, \infty)$. This can be written as:

$$\hat{f}(x) = \sum_{j=1}^q (x - j + 1)_+ a_j + f(0)$$

with $a_1 = f(1) - f(0)$, $a_{j+1} = f(j+1) - 2f(j) + f(j-1)$ (implying $a_q = -\infty$). It is easy to see that $h = \hat{f} \otimes \hat{g}$ coincides with the discrete convolution of f and g in its (discrete) domain; the reason is simply that h is also piecewise-linear, with kinks only in discrete values $\{0, \dots, 2(q-1)\}$.

When computing the convolution of N functions f_1, \dots, f_N with domain in $\{0, \dots, q-1\}$, one can clearly order all slopes together in one initial pass, using $Nq \log(Nq)$ comparisons. It is also easy to see that, if one has the full convolution, it is simple to compute a ‘‘cavity’’ convolution in which one function f_i is omitted, in $O(q)$ time: this is achieved by simply removing the q slopes of f_i from the full convolution.

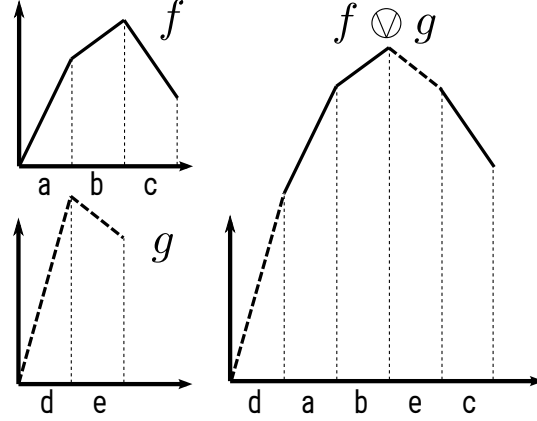


FIG. 1. Sketch of the discrete max-convolution $f \otimes g$ of piecewise-linear concave functions f, g . The result is simply obtained by sorting the pieces of the two functions in descending order of slope.

In order to apply this to eq. (10) the only remaining step is a trivial affine mapping of the functions arguments $W_j \xi_j^t$ on a domain $\{A + tB : t \in \{0, \dots, q-1\}\}$ to the domain $\{0, \dots, q-1\}$. In the following, we will show explicitly how to do this for the binary case $q = 2$, but the argument can be easily generalized to arbitrary q . Note that, while in the binary case the Ψ functions are linear and thus trivially concave, in the general case we need to ensure that both the initial values $\Phi_{i \rightarrow \mu}^0(W_i)$ and the external fields $\Gamma_i(W_i)$ are concave; in such case, the iteration equations (3), (7) and (8) ensure that the concavity property holds for all time steps $t > 0$.

B. The binary case

We will show explicitly how to perform efficiently the computations for the binary case. In this case we can simplify the notation by parametrizing the message with a single scalar, i.e. we can write $\Phi_{\mu \rightarrow i}^t(W_i) = W_i \phi_{\mu \rightarrow i}^t$ and $\Psi_{i \rightarrow \mu}^t(W_i) = W_i \psi_{i \rightarrow \mu}^t$ and $\Gamma_i(W_i) = W_i \gamma_i$. Eqs. (3) and (7) then become:

$$\phi_{\mu \rightarrow i}^{t+1} = \frac{1}{2} \left(\max_{\mathbf{w}: W_i = 1 \wedge E_\mu(W) = 0} \sum_{j \neq i} W_j \psi_{j \rightarrow \mu}^t - \max_{\mathbf{w}: W_i = -1 \wedge E_\mu(W) = 0} \sum_{j \neq i} W_j \psi_{j \rightarrow \mu}^t \right) \quad (12)$$

$$\psi_{i \rightarrow \mu}^t = r t \psi_i^{t-1} + \gamma_i + \sum_{\mu' \neq \mu} \phi_{\mu' \rightarrow i}^t \quad (13)$$

Correspondingly, eqs. (8) and (6) simplify to:

$$\psi_i^t = r^t \psi_i^{t-1} + \gamma_i + \sum_{\mu} \phi_{\mu \rightarrow i}^t \quad (14)$$

$$W_i^t = \text{sign} \psi_i^t \quad (15)$$

In order to apply the results of the previous sections, and perform efficiently the trace over all possible assignments of W of eq. (12), we first introduce the auxiliary quantities

$$F_{\mu}^t(\mathbf{S}) = \sum_i S_i \xi_i^{\mu} \psi_{i \rightarrow \mu}^t \quad (16)$$

$$\mathcal{F}_{\mu}^t(\Delta) = \max_{\{\mathbf{S}: \sum_i S_i = \Delta\}} F_{\mu}^t(\mathbf{S}) \quad (17)$$

For simplicity of notation, we will temporarily drop the indices μ and t . We will also assume that all values $\psi_{i \rightarrow \mu}^t$ are different: as remarked above, the presence of term Γ_i is sufficient to ensure that this is the case, and otherwise we can impose an arbitrary order without loss of generality. With this assumption, the function \mathcal{F} , which is defined over $\Delta = \{-N, -N+2, \dots, N-2, N\}$, has a single absolute maximum, and is indeed concave. The absolute maximum is obtained with the special configuration $\tilde{\mathbf{S}} = \text{argmax}_{\{S_i\}} F(\mathbf{S})$, which is trivially obtained by setting $\tilde{S}_i = \xi_i^{\mu} \text{sign} \psi_{i \rightarrow \mu}^t$ for all i . This configuration corresponds to a value $\tilde{\Delta} = \sum_i \tilde{S}_i$. Any variable flip with respect to this configuration, i.e. any i for which $S_i = -\tilde{S}_i$, adds a “cost” $\Delta F_i = 2 \left| \psi_{i \rightarrow \mu}^t \right|$ in terms of $F(\mathbf{S})$. Therefore, if we partition the indices i in two groups S_+ and S_- defined by $S_{\pm} = \{i : \tilde{S}_i = \pm 1\}$, and we sort the indices within each group in ascending order according to ΔF_i , we can compute the function $\mathcal{F}(\Delta)$ for each Δ by constructively computing the corresponding optimal configuration \mathbf{S} , in the following way: we start from $\mathcal{F}(\tilde{\Delta})$, then proceed in steps of 2 in both directions subtracting the values ΔF_i in ascending order, using the variable indices in S_+ for $\Delta < \tilde{\Delta}$ and those in S_- for $\Delta > \tilde{\Delta}$.

This procedure also associates a “turning point” T_i to each index i , defined as the value of Δ for which the optimal value of W_i changes sign, or equivalently such that $\mathcal{F}(T_i + \tilde{S}_i) - \mathcal{F}(T_i - \tilde{S}_i) = \Delta F_i$. This also implies that:

$$\mathcal{F}(\Delta) = \mathcal{F}(\tilde{\Delta}) - \sum_i \Theta(\tilde{S}_i(T_i - \Delta)) \Delta F_i \quad (18)$$

We can also bijectively associate an index to each value of T_i , by defining j_k such that $T_{j_k} = k$.

Next, consider the same quantity where a variable i is left out of the sum (see eq. (10))

$$F^{(i)}(\mathbf{S}^{(i)}) = \sum_{j \neq i} S_j \xi_j^\mu \psi_{j \rightarrow \mu}^t \quad (19)$$

$$\mathcal{F}^{(i)}(\Delta) = \max_{\{S_j\}_{j \neq i}: \sum_{j \neq i} S_j = \Delta} F^{(i)}(\mathbf{S}^{(i)}) \quad (20)$$

Clearly, one gets the same overall picture as before, except with a shifted argmax, and shifted turning points. The shifts can be easily expressed in terms of the previous quantities, and the expressions used for computing eq. (12) as:

$$\phi_{\mu \rightarrow i}^{t+1} = \frac{\xi_i^\mu}{2} \left(\max_{\Delta: \sigma_D^\mu \Delta > 0} \mathcal{F}^{(i)}(\Delta - 1) - \max_{\Delta: \sigma_D^\mu \Delta > 0} \mathcal{F}^{(i)}(\Delta + 1) \right) \quad (21)$$

The full details of the computation are provided in the Appendix, Sec. V. Here, we report the end result:

$$\begin{aligned} \phi_{\mu \rightarrow i}^{t+1} = \xi_i^\mu & \left(\Theta(\sigma_D^\mu) \Theta(-\tilde{\Delta} + \tilde{S}_i + 1) (\Theta(T_i - 1) h_{j_0} + \Theta(-T_i + 1) h_{j_2}) + \right. \\ & \left. + \Theta(-\sigma_D^\mu) \Theta(\tilde{\Delta} - \tilde{S}_i + 1) (\Theta(T_i + 1) h_{j_{-2}} + \Theta(-T_i - 1) h_{j_0}) \right) \end{aligned} \quad (22)$$

where $h_j = -\xi_j^\mu \psi_{j \rightarrow \mu}^t$. From this expression, we see that we can update the cavity fields $\phi_{\mu \rightarrow i}$ very efficiently for all i , using the following procedure:

- We do one pass of the whole array of h_i by which we determine the \tilde{S}_i values, we split the indices j into S_+ and S_- and we compute $\tilde{\Delta}$. This requires $\mathcal{O}(N)$ operations (all of which are trivial).
- We separately partially sort the indices in S_+ and S_- and get j_{-2} , j_0 and j_2 and the turning points T_i . This requires at most $\mathcal{O}(N \log N)$ operations. Note that we can use a partial sort because we computed $\tilde{\Delta}$, and so we know how many indices we need to sort, and from which set S_\pm , until we get to the ones with turning points around 0; also, we are only interested in computing $\Theta(T_i - 1)$ and $\Theta(T_i + 1)$ instead of all values of T_i . This makes it likely for the procedure to be significantly less computationally expensive than the worst case scenario.
- For each i we compute $\phi_{\mu \rightarrow i}^{t+1}$ from the equation above. This requires $\mathcal{O}(1)$ operations (implemented in practice with three conditionals and a lookup).

IV. NUMERICAL RESULTS

We tested extensively the binary case $q = 2$ with $W_i \in \{-1, +1\}$ and the ternary case $q = 3$ with $W_i \in \{-1, 0, 1\}$, for single layer networks.

We start from the binary case. Fig. 2 shows the probability of finding a solution when fixing the reinforcement rate r , for different values of r and α . Reducing r allows to reach higher values of α ; the shape of the curves suggest that in the limit $r \rightarrow 0$ there would be sharp transitions at critical values of α 's. In the classification case, Fig. 2A, the transition is around $\alpha \simeq 0.75$, while the theoretical critical capacity is $\alpha_c = 0.83$. This value is comparable to the one obtained with the reinforced BP algorithm of [14]. In the generalization case, there are two transitions: the first one occurs around $\alpha \simeq 1.1$, before the first-order transition at $\alpha_{TS} = 1.245$ where, according to the theory, the only solution is the teacher; the second transition occurs around $\alpha \simeq 1.5$. This second transition is compatible with the end of the meta-stable regime (see e.g. [2]); indeed, after this point the algorithm is able to correctly infer the teacher perceptron.

A second batch of experiments on the same architecture, in the classification case, is shown in Fig. 3. In this case, we estimated the maximum value of r which allows to find a solution, at different values of N and α ; i.e. for each test sample we started from a high value of r (e.g. $r = 10^{-1}$) and checked if the algorithm was able to find a solution; if the algorithm failed, we reduced r and tried the same sample again. In the cases shown, the solution was always found eventually. The results indicate that the value of r required decreases with N , and the behaviour is well described by a power law, i.e. $r = aN^b$ with $a < 0$ and $b < 0$, where the values of a and b depend on α . Since the number of iterations required is inversely proportional to r (not shown), this implies that the overall solving time of the MS algorithm is of $O(N^{1-b} \log(N))$, i.e. it is worse than the reinforced BP in this respect. The value of b is between 0 and -0.5 up to $\alpha = 0.6$, after which its magnitude decreases abruptly (see Fig. 3B). The behaviour for large α seems to be reasonably well fit by a curve $b(\alpha) = \frac{c}{\alpha_U - \alpha}$, suggesting the presence of a vertical asymptote at $\alpha_U = 0.755 \pm 0.004$, which is an estimate of the critical capacity of the algorithm in the limit of large N .

In the ternary single layer case, we tested learning of $\{-1, 1\}$ random patterns with ternary $\{-1, 0, 1\}$

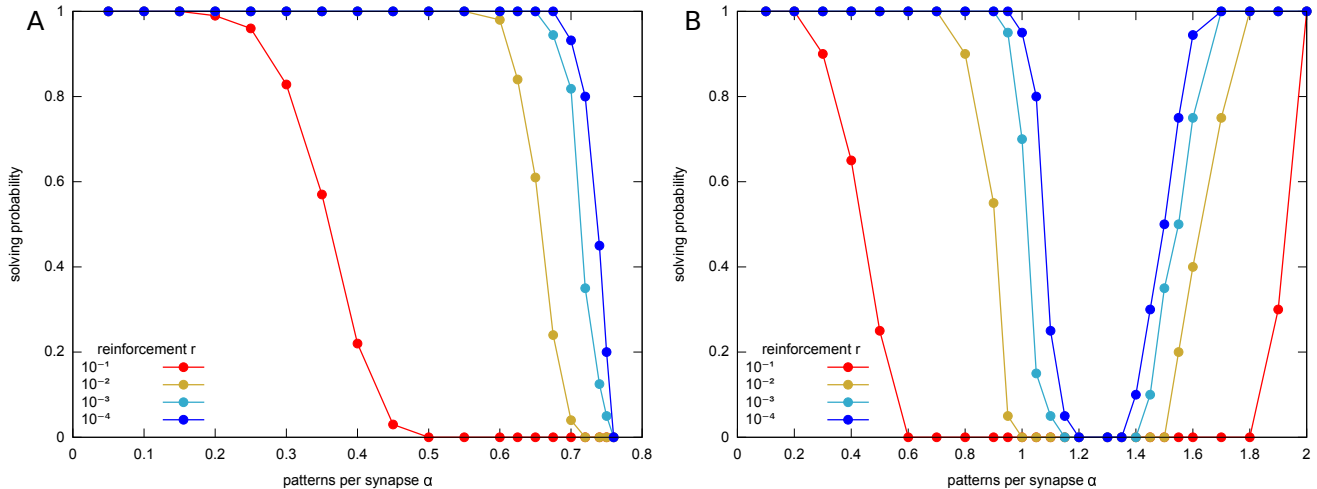


FIG. 2. **Solving probability.** Probability of finding a solution for different values of α , in the binary perceptron case with $N = 1001$, with different values of the reinforcement rate parameter r . Performance improves with lower values of r . **A.** Classification case, 100 samples per point. The theoretical capacity is $\alpha_c = 0.83$ in this case. **B.** Generalization case, 20 samples per point. In this case, the problem has multiple solutions up to $\alpha_{TS} = 1.245$, after which the only solution is the teacher.

weights and concave bias (i.e. prior). In practice, we use the function $\Gamma_i(W_i) = \lambda\delta(W_i) + \Gamma'_i(W_i)$ (where Γ' is the symmetry-breaking noise term and λ is sufficiently large) to favour zero weights, so solutions with a minimal number of zeros are searched, i.e. we add an l_0 regularization term. Results (See Fig. 4) are qualitatively similar to the $\{-1, 1\}$ case with a larger capacity (around $\alpha = 1$; the critical capacity is $\alpha_c = 1.17$ in this case). The average non-zero weights in a solution grows when getting closer to the critical α up to a value that is smaller than $2/3$ (the value that makes the entropy of unconstrained $\{-1, 0, 1\}$ perceptrons largest).

In the fully-connected multi-layer case, the algorithm does not get as close to the critical capacity as for the single-layer case, but it is still able to achieve non-zero capacity in rather large instances. For example, in the classification case with binary synapses, $N = 1001$ inputs, $K = 3$ hidden units, the algorithmic critical capacity is $\alpha \simeq 0.33$ when $r = 10^{-5}$ (tested on 20 samples), corresponding to storing $M = 1001$ patterns with 3003 weights (thus demonstrating a greater discriminatory power than

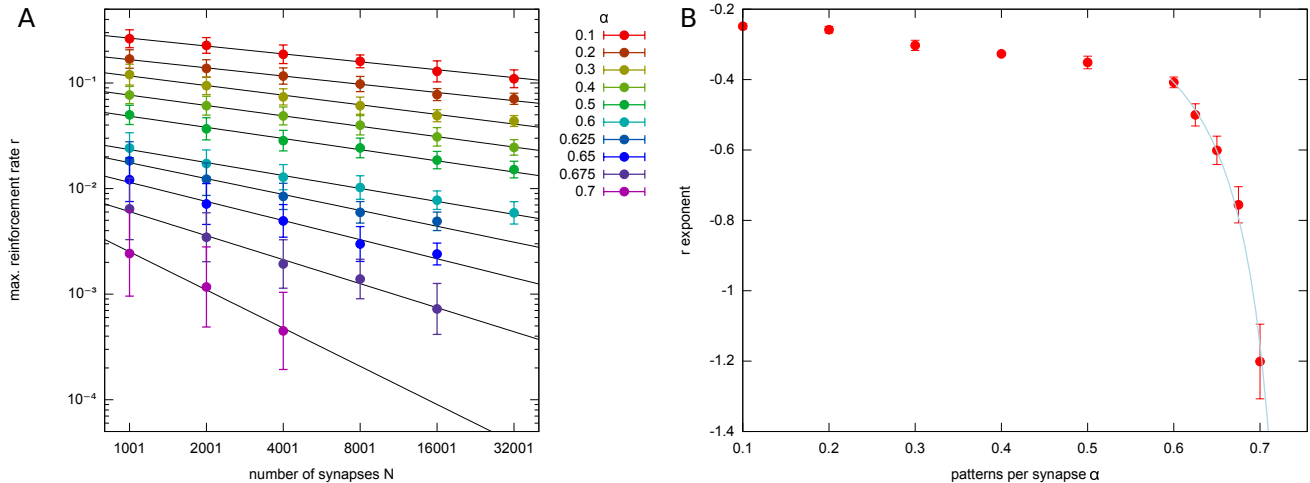


FIG. 3. **Maximum reinforcement rate.** **A.** Average value of the maximum reinforcement rate r which allows to find a solution, in the binary perceptron classification case, at various values of N and α , in log-log scale. The reinforcement rate decreases with N and α . Error bars show the standard deviation of the distributions. Black lines show the result of fits of the form $r(\alpha, N) = a(\alpha) N^{b(\alpha)}$, one for each value of α . The number of samples varied between 100 for $N = 1001$ and 10 for $N = 32001$. **B.** The fitted values of the exponents $b(\alpha)$ in panel A. The continuous curve shows a fit of the data for $\alpha \geq 0.6$ by the function $b(\alpha) = \frac{c}{\alpha_U - \alpha}$. The fit yields $c = -0.063 \pm 0.002$ and $\alpha_U = 0.755 \pm 0.004$. The value of α_U is an estimate of the critical capacity of the algorithm.

the single-layer case with the same input size). The reason for the increased difficulty in this case is not completely clear: we speculate that it is both due to the permutation symmetry between the hidden units and to replica-symmetry-breaking effects: these effects tend to trap the algorithm — in its intermediate steps — in states which mix different clusters of solutions, making convergence difficult. Still, the use of symmetry-breaking noise helps achieving non trivial results even in this case, which constitutes an improvement with respect to the standard BP algorithm.

V. CONCLUSIONS

Up to now, the large N limit could be exploited on BP equations for the learning problem with discrete synapses to obtain an extremely simple set of approximated equations that made the computation

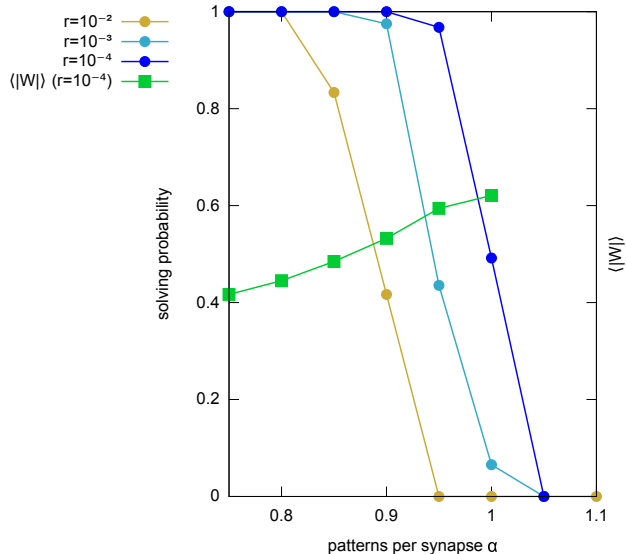


FIG. 4. Learning of random $\{-1, 1\}$ patterns with a ternary $w = \{-1, 0, 1\}$ perceptron, with dilution (regularization) prior term; $N = 1001$, 20 samples per point. For solved instances with $r = 10^{-4}$, the average fraction of non-zero weights is also shown (standard deviations smaller than point size).

of an iteration to scale linearly with the problem size MN . For the MS equations however, those approximations cannot be made and a naive approximation scales as MN^3 which is normally too slow for most practical purposes. In this work, we showed that MS equations can be computed exactly (with no approximations) in time $MN \log N$, rendering the approach extremely interesting in practice. A word is in order about the MS equations with reinforcement term, which we propose as a valid alternative to Belief Propagations-based methods. Although we cannot claim any universal property of the reinforced equations from theoretical arguments and we only tested a limited number of cases, extensive simulations for these cases and previous results obtained by applying the same technique to other optimization problems of very different nature [22, 28–30] have confirmed the same qualitative behaviour; that is, that the number of iterations until convergence scales as r^{-1} and that results monotonically improve as r decreases. As an additional advantage of MS, inherent symmetries present in the original system are naturally broken thanks to ad-hoc noise terms that are standard in MS. The MS equations are additionally

computationally simpler because they normally require only sum and max operations, in contrast with hyperbolic trigonometric functions required by BP equations. Extensive simulations for discrete $\{-1, 1\}$ and $\{-1, 0, 1\}$ weights show that the performance is indeed very good, and the algorithm achieves a capacity close to the theoretical one (very similar to the one of Belief Propagation).

ACKNOWLEDGMENTS

CB acknowledges the European Research Council for grant n° 267915.

APPENDIX

Details of the computation of the cavity fields.

In this section we provide the full details of the computation leading to eq. (22).

As noted in the main text, the expression of the cavity quantities $\mathcal{F}^{(i)}(\Delta)$ (see eq. (20)) is analogous to that of the non-cavity counterpart $\mathcal{F}(\Delta)$ (eq. (18)), where the argmax has changed to $\tilde{\Delta}^{(i)} = \tilde{\Delta} - \tilde{S}_i$, and the turning points have changed:

$$\mathcal{F}^{(i)}(\Delta) = \mathcal{F}^{(i)}(\tilde{\Delta}^{(i)}) - \sum_{j \neq i} \Theta\left(\tilde{S}_j \left(T_j^{(i)} - \Delta\right)\right) \Delta F_j \quad (23)$$

We need to express the relationship between the old turning points and the new ones: having omitted the variable i , it means that there is a global shift of $-\tilde{S}_i$, and that the turning points to the left (right) of T_i have shifted to the right (left) if $\tilde{S}_i = 1$ ($\tilde{S}_i = -1$, respectively):

$$\begin{aligned} T_j^{(i)} &= T_j - \tilde{S}_i + 2\tilde{S}_i \Theta\left(\tilde{S}_i (T_i - T_j)\right) \\ &= T_j + \text{sign}\left(T_i - T_j - \tilde{S}_i\right) \end{aligned} \quad (24)$$

(note that we chose to use the convention that $\Theta(0) = 0$).

Therefore we obtain:

$$\mathcal{F}^{(i)}(\Delta) = \mathcal{F}^{(i)}(\tilde{\Delta}^{(i)}) - \sum_{j \neq i} \Theta\left(\tilde{S}_j \left(T_j + \text{sign}\left(T_i - T_j - \tilde{S}_i\right) - \Delta\right)\right) \Delta F_j \quad (25)$$

Next, we consider the cavity quantity:

$$\begin{aligned} \mathcal{C}_i(\Delta, S_i) &= \max_{\{S_j\}_{j \neq i}: \sum_j S_j \xi_j^\mu = \Delta} \left(\sum_{j \neq i} S_j \xi_j^\mu \psi_{j \rightarrow \mu}^t \right) \\ &= \mathcal{F}^{(i)}(\Delta - S_i) \end{aligned} \quad (26)$$

which allows us to write eq. (12) as

$$\begin{aligned} \phi_{\mu \rightarrow i}^{t+1} &= \frac{\xi_i^\mu}{2} \left(\max_{\Delta: \sigma_D^\mu \Delta > 0} \mathcal{C}_i(\Delta, \xi_i^\mu) - \max_{\Delta: \sigma_D^\mu \Delta > 0} \mathcal{C}_i(\Delta, -\xi_i^\mu) \right) \\ &= \frac{\xi_i^\mu}{2} \left(\max_{\Delta: \sigma_D^\mu \Delta > 0} \mathcal{F}^{(i)}(\Delta - 1) - \max_{\Delta: \sigma_D^\mu \Delta > 0} \mathcal{F}^{(i)}(\Delta + 1) \right) \end{aligned} \quad (27)$$

(this is eq. (21) in the main text).

Note that $\mathcal{F}^{(i)}(\Delta)$ is concave and has a maximum at $\tilde{\Delta}^{(i)} = \tilde{\Delta} - \tilde{S}_i$. Using this fact, and eq. (25), we can derive explicit formulas for the expressions which appear in the cavity field, by considering the two cases for σ_D^μ separately, and simplifying the result with simple algebraic manipulations afterwards:

$$\begin{aligned} \max_{\Delta: \sigma_D^\mu \Delta > 0} \mathcal{F}^{(i)}(\Delta - 1) &= \Theta(\sigma_D^\mu) \left(\Theta(\tilde{\Delta} - \tilde{S}_i + 1) \mathcal{F}^{(i)}(\tilde{\Delta} - \tilde{S}_i) + \Theta(-\tilde{\Delta} + \tilde{S}_i - 1) \mathcal{F}^{(i)}(0) \right) + \\ &\quad + \Theta(-\sigma_D^\mu) \left(\Theta(-\tilde{\Delta} + \tilde{S}_i - 1) \mathcal{F}^{(i)}(\tilde{\Delta} - \tilde{S}_i) + \Theta(\tilde{\Delta} - \tilde{S}_i + 1) \mathcal{F}^{(i)}(-2) \right) \\ &= \Theta(\sigma_D^\mu (\tilde{\Delta} - \tilde{S}_i + 1)) \mathcal{F}^{(i)}(\tilde{\Delta} - \tilde{S}_i) + \\ &\quad + \Theta(\sigma_D^\mu) \Theta(-\tilde{\Delta} + \tilde{S}_i - 1) \mathcal{F}^{(i)}(0) + \\ &\quad + \Theta(-\sigma_D^\mu) \Theta(\tilde{\Delta} - \tilde{S}_i + 1) \mathcal{F}^{(i)}(-2) \end{aligned}$$

$$\begin{aligned} \max_{\Delta: \sigma_D^\mu \Delta > 0} \mathcal{F}^{(i)}(\Delta + 1) &= \Theta(\sigma_D^\mu) \left(\Theta(\tilde{\Delta} - \tilde{S}_i - 1) \mathcal{F}^{(i)}(\tilde{\Delta} - \tilde{S}_i) + \Theta(-\tilde{\Delta} + \tilde{S}_i + 1) \mathcal{F}^{(i)}(2) \right) + \\ &\quad + \Theta(-\sigma_D^\mu) \left(\Theta(-\tilde{\Delta} + \tilde{S}_i + 1) \mathcal{F}^{(i)}(\tilde{\Delta} - \tilde{S}_i) + \Theta(\tilde{\Delta} - \tilde{S}_i - 1) \mathcal{F}^{(i)}(0) \right) \\ &= \Theta(\sigma_D^\mu (\tilde{\Delta} - \tilde{S}_i - 1)) \mathcal{F}^{(i)}(\tilde{\Delta} - \tilde{S}_i) + \\ &\quad + \Theta(\sigma_D^\mu) \Theta(-\tilde{\Delta} + \tilde{S}_i + 1) \mathcal{F}^{(i)}(2) + \\ &\quad + \Theta(-\sigma_D^\mu) \Theta(\tilde{\Delta} - \tilde{S}_i - 1) \mathcal{F}^{(i)}(0) \end{aligned}$$

Plugging these back in the expression for the cavity field, we can reach — again by simple algebraic manipulations — an expression which only uses $\mathcal{F}^{(i)}(-2)$, $\mathcal{F}^{(i)}(0)$ and $\mathcal{F}^{(i)}(2)$:

$$\begin{aligned}
\phi_{\mu \rightarrow i}^{t+1} &= \frac{\xi_i^\mu}{2} \left(\left(\Theta \left(\sigma_D^\mu \left(\tilde{\Delta} - \tilde{S}_i + 1 \right) \right) - \Theta \left(\sigma_D^\mu \left(\tilde{\Delta} - \tilde{S}_i - 1 \right) \right) \right) \mathcal{F}^{(i)} \left(\tilde{\Delta} - \tilde{S}_i \right) + \right. \\
&\quad \left. + \Theta \left(\sigma_D^\mu \right) \left(\Theta \left(-\tilde{\Delta} + \tilde{S}_i - 1 \right) \mathcal{F}^{(i)}(0) - \Theta \left(-\tilde{\Delta} + \tilde{S}_i + 1 \right) \mathcal{F}^{(i)}(2) \right) + \right. \\
&\quad \left. + \Theta \left(-\sigma_D^\mu \right) \left(\Theta \left(\tilde{\Delta} - \tilde{S}_i + 1 \right) \mathcal{F}^{(i)}(-2) - \Theta \left(\tilde{\Delta} - \tilde{S}_i - 1 \right) \mathcal{F}^{(i)}(0) \right) \right) \\
&= \frac{\xi_i^\mu}{2} \left(\delta \left(\tilde{\Delta}, \tilde{S}_i \right) \text{sign} \left(\sigma_D^\mu \right) \mathcal{F}^{(i)}(0) + \right. \\
&\quad \left. + \Theta \left(\sigma_D^\mu \right) \left(-\delta \left(\tilde{\Delta}, \tilde{S}_i \right) \mathcal{F}^{(i)}(2) + \Theta \left(-\tilde{\Delta} + \tilde{S}_i - 1 \right) \left(\mathcal{F}^{(i)}(0) - \mathcal{F}^{(i)}(2) \right) \right) + \right. \\
&\quad \left. + \Theta \left(-\sigma_D^\mu \right) \left(\delta \left(\tilde{\Delta}, \tilde{S}_i \right) \mathcal{F}^{(i)}(-2) + \Theta \left(\tilde{\Delta} - \tilde{S}_i - 1 \right) \left(\mathcal{F}^{(i)}(-2) - \mathcal{F}^{(i)}(0) \right) \right) \right) \\
&= \frac{\xi_i^\mu}{2} \left(\delta \left(\tilde{\Delta}, \tilde{W}_i \xi_i^\mu \right) \left(\text{sign} \left(\sigma_D^\mu \right) \left(\mathcal{F}^{(i)}(0) - \mathcal{F}^{(i)}(2\sigma_D^\mu) \right) \right) + \right. \\
&\quad \left. + \Theta \left(\sigma_D^\mu \right) \Theta \left(-\tilde{\Delta} + \tilde{W}_i \xi_i^\mu - 1 \right) \left(\mathcal{F}^{(i)}(0) - \mathcal{F}^{(i)}(2) \right) + \right. \\
&\quad \left. + \Theta \left(-\sigma_D^\mu \right) \Theta \left(\tilde{\Delta} - \tilde{W}_i \xi_i^\mu - 1 \right) \left(\mathcal{F}^{(i)}(-2) - \mathcal{F}^{(i)}(0) \right) \right) \\
&= \frac{\xi_i^\mu}{2} \left(\Theta \left(\sigma_D^\mu \right) \Theta \left(-\tilde{\Delta} + \tilde{S}_i + 1 \right) \left(\mathcal{F}^{(i)}(0) - \mathcal{F}^{(i)}(2) \right) + \right. \\
&\quad \left. + \Theta \left(-\sigma_D^\mu \right) \Theta \left(\tilde{\Delta} - \tilde{S}_i + 1 \right) \left(\mathcal{F}^{(i)}(-2) - \mathcal{F}^{(i)}(0) \right) \right)
\end{aligned}$$

These expressions can be further simplified, since the differences between the values of $\mathcal{F}^{(i)}$ at neighboring values only depends on the “steps” induced by the spins which are associated with turning points in that region:

$$\begin{aligned}
\mathcal{F}^{(i)}(0) - \mathcal{F}^{(i)}(2) &= \sum_{j \neq i} \left(\Theta \left(\tilde{S}_j \left(T_j + \text{sign} \left(T_i - T_j - \tilde{S}_i \right) - 2 \right) \right) - \Theta \left(\tilde{S}_j \left(T_j + \text{sign} \left(T_i - T_j - \tilde{S}_i \right) \right) \right) \right) \Delta F_j \\
&= - \sum_{j \neq i} \tilde{S}_j \delta \left(T_j, 1 - \text{sign} \left(T_i - T_j - \tilde{S}_i \right) \right) \Delta F_j \\
&= -\tilde{S}_{j_0} (1 - \delta(i, j_0)) \Theta \left(T_i - \tilde{S}_i \right) \Delta F_{j_0} - \tilde{S}_{j_2} (1 - \delta(i, j_2)) \Theta \left(-T_i + 2 + \tilde{S}_i \right) \Delta F_{j_2} \\
&= -\tilde{S}_{j_0} \Theta(T_i - 1) \Delta F_{j_0} - \tilde{S}_{j_2} \Theta(-T_i + 1) \Delta F_{j_2}
\end{aligned}$$

where in the last step we used the Kronecker deltas to get rid for the differences between the two cases for \tilde{S}_i . The other case is very similar:

$$\begin{aligned}
\mathcal{F}^{(i)}(-2) - \mathcal{F}^{(i)}(0) &= \sum_{j \neq i} \left(\Theta \left(\tilde{S}_j \left(T_j + \text{sign} \left(T_i - T_j - \tilde{S}_i \right) \right) \right) - \Theta \left(\tilde{S}_j \left(T_j + \text{sign} \left(T_i - T_j - \tilde{S}_i \right) + 2 \right) \right) \right) \Delta F_j \\
&= - \sum_{j \neq i} \tilde{S}_j \delta \left(T_j, -1 - \text{sign} \left(T_i - T_j - \tilde{S}_i \right) \right) \Delta F_j \\
&= -\tilde{S}_{j_{-2}} (1 - \delta(i, j_{-2})) \Theta \left(T_i + 2 - \tilde{S}_i \right) \Delta F_{j_{-2}} - \tilde{S}_{j_0} (1 - \delta(i, j_0)) \Theta \left(\tilde{S}_i - T_i \right) \Delta F_{j_0} \\
&= -\tilde{S}_{j_{-2}} \Theta \left(T_i + 1 \right) \Delta F_{j_{-2}} - \tilde{S}_{j_0} \Theta \left(-1 - T_i \right) \Delta F_{j_0}
\end{aligned}$$

Going back to the cavity fields, and defining $h_j = -\frac{1}{2}\tilde{S}_j\Delta F_j = -\xi_j^\mu\psi_{j \rightarrow \mu}^t$, we finally get eq. (22):

$$\begin{aligned}
\phi_{\mu \rightarrow i}^{t+1} &= \xi_i^\mu \left(\Theta \left(\sigma_D^\mu \right) \Theta \left(-\tilde{\Delta} + \tilde{S}_i + 1 \right) \left(\Theta \left(T_i - 1 \right) h_{j_0} + \Theta \left(-T_i + 1 \right) h_{j_2} \right) + \right. \\
&\quad \left. + \Theta \left(-\sigma_D^\mu \right) \Theta \left(\tilde{\Delta} - \tilde{S}_i + 1 \right) \left(\Theta \left(T_i + 1 \right) h_{j_{-2}} + \Theta \left(-T_i - 1 \right) h_{j_0} \right) \right)
\end{aligned}$$

-
- [1] David E. Rumelhart, Geoffrey E. Hinton, and Ronald J. Williams. Learning representations by back-propagating errors. *Nature*, 323(6088):533–536, October 1986.
 - [2] A Engel and C. van den Broeck. *Statistical mechanics of learning*. Cambridge University Press, Cambridge, UK; New York, NY, 2001.
 - [3] Edoardo Amaldi, Eddy Mayoraz, and Dominique de Werra. A review of combinatorial problems arising in feedforward neural network design. *Discrete Applied Mathematics*, 52(2):111–138, 1994.
 - [4] Avrim L Blum and Ronald L Rivest. Training a 3-node neural network is np-complete. *Neural Networks*, 5(1):117–127, 1992.
 - [5] Carl CH Petersen, Robert C Malenka, Roger A Nicoll, and John J Hopfield. All-or-none potentiation at ca3-ca1 synapses. *Proceedings of the National Academy of Sciences*, 95(8):4732–4737, 1998.
 - [6] Daniel H O’Connor, Gayle M Wittenberg, and Samuel S-H Wang. Graded bidirectional synaptic plasticity is composed of switch-like unitary events. *Proceedings of the National Academy of Sciences of the United States of America*, 102(27):9679–9684, 2005.

- [7] Thomas M Bartol, Cailey Bromer, Justin P Kinney, Michael A Chirillo, Jennifer N Bourne, Kristen M Harris, and Terrence J Sejnowski. Hippocampal spine head sizes are highly precise. *bioRxiv*, 2015.
- [8] Upinder S Bhalla and Ravi Iyengar. Emergent properties of networks of biological signaling pathways. *Science*, 283(5400):381–387, 1999.
- [9] William Bialek. Stability and noise in biochemical switches. *Advances in neural information processing systems*, pages 103–109, 2001.
- [10] Arnold Hayer and Upinder S Bhalla. Molecular switches at the synapse emerge from receptor and kinase traffic. *PLoS computational biology*, 1(2):e20, 2005.
- [11] Paul Miller, Anatol M Zhabotinsky, John E Lisman, and Xiao-Jing Wang. The stability of a stochastic camkii switch: dependence on the number of enzyme molecules and protein turnover. *PLoS biology*, 3(4):e107, 2005.
- [12] Werner Krauth and Marc Mézard. Storage capacity of memory networks with binary couplings. *Journal de Physique*, 50(20):3057–3066, 1989.
- [13] Haiping Huang and Yoshiyuki Kabashima. Origin of the computational hardness for learning with binary synapses. *Physical Review E*, 90(5):052813, November 2014.
- [14] Alfredo Braunstein and Riccardo Zecchina. Learning by message passing in networks of discrete synapses. *Physical Review Letters*, 96(3):030201, January 2006.
- [15] Marc Mézard and Andrea Montanari. *Information, Physics, and Computation*. Oxford University Press, January 2009.
- [16] Carlo Baldassi, Alfredo Braunstein, Nicolas Brunel, and Riccardo Zecchina. Efficient supervised learning in networks with binary synapses. *Proceedings of the National Academy of Sciences*, 104(26):11079–11084, June 2007.
- [17] Carlo Baldassi. Generalization learning in a perceptron with binary synapses. *Journal of Statistical Physics*, 136, September 2009.
- [18] Frank Rosenblatt. The perceptron: a probabilistic model for information storage and organization in the brain. *Psychological review*, 65(6):386, 1958.
- [19] Nils J Nilsson. *Learning machines*. New York, McGrawHill, 1965.
- [20] A Engel, HM Köhler, F Tschepeke, H Vollmayr, and A Zippelius. Storage capacity and learning algorithms for two-layer neural networks. *Physical Review A*, 45(10):7590, 1992.
- [21] Yoshiyuki Kabashima. A CDMA multiuser detection algorithm on the basis of belief propagation. *Journal of Physics A: Mathematical and General*, 36(43):11111, October 2003.
- [22] M. Bailly-Bechet, C. Borgs, A. Braunstein, J. Chayes, A. Dagkessamanskaia, J.-M. François, and R. Zecchina.

- Finding undetected protein associations in cell signaling by belief propagation. *Proceedings of the National Academy of Sciences*, 108(2):882–887, January 2011.
- [23] Alfredo Braunstein, Roberto Mulet, and Andrea Pagnani. Estimating the size of the solution space of metabolic networks. *BMC Bioinformatics*, 9(1):240, May 2008.
- [24] A. Braunstein, F. Kayhan, and R. Zecchina. Efficient data compression from statistical physics of codes over finite fields. *Physical Review E*, 84(5):051111, November 2011.
- [25] Alfredo Braunstein, Farbod Kayhan, and Riccardo Zecchina. Efficient LDPC codes over $\text{GF}(q)$ for lossy data compression. In *IEEE International Symposium on Information Theory, 2009. ISIT 2009*, Seoul, Korea, 2009.
- [26] Jean-Yves Le Boudec and Patrick Thiran. *Network Calculus: A Theory of Deterministic Queuing Systems for the Internet*. Springer Science & Business Media, July 2001.
- [27] We allow $a_{k_i}^i = -\infty$, in which case we conventionally define $a_{k_i}^i y_+ = 0$ if $y \leq 0$.
- [28] Anthony Gitter, Alfredo Braunstein, Andrea Pagnani, Carlo Baldassi, Christian Borgs, Jennifer Chayes, Riccardo Zecchina, and Ernest Fraenkel. Sharing information to reconstruct patient-specific pathways in heterogeneous diseases. In *Pacific Symposium on Biocomputing 2014*, pages 39–50. World Scientific, 2013.
- [29] F. Altarelli, A. Braunstein, L. Dall’Asta, and R. Zecchina. Optimizing spread dynamics on graphs by message passing. *Journal of Statistical Mechanics: Theory and Experiment*, 2013(09):P09011, September 2013.
- [30] F. Altarelli, A. Braunstein, L. Dall’Asta, J. R. Wakeling, and R. Zecchina. Containing Epidemic Outbreaks by Message-Passing Techniques. *Physical Review X*, 4(2):021024, May 2014.